Available online at www.sciencedirect.com
ScienceDirect
Solar Energy Materials & Solar Cells 91 (2007) 160–166
Solar Energy Materials and Solar Cells
www.elsevier.com/locate/solmat

A detailed study of p–n junction solar cells by means of collection efficiency

P. Kittidachachan[a,*], T. Markvart[a], D.M. Bagnall[b], R. Greef[c], G.J. Ensell[d]

[a]*Materials Research Group, School of Engineering Sciences, University of Southampton, Highfield, Southampton SO17 1BJ, UK*
[b]*Nanoscale Systems Integration Group, School of Electronics and Computer Science, University of Southampton, Highfield, Southampton SO17 1BJ, UK*
[c]*School of Chemistry, University of Southampton, Highfield, Southampton SO17 1BJ, UK*
[d]*Nanoscale Systems Integration Group and Innos Ltd., University of Southampton, Highfield, Southampton SO17 1BJ, UK*

Received 16 March 2006; accepted 8 August 2006
Available online 27 September 2006

Abstract

The operation of a crystalline silicon solar cell was studied by a methodology based on collection efficiency. The collection efficiencies of the base, emitter, and depletion layers were determined separately using numerical solutions. The quantum efficiency was then determined by the reciprocity theorem. It is shown that the model can provide useful new insights and can be used to extract device parameters by fitting the modelled results to experimental data.

Keywords: Collection efficiency; Spectral response; Quantum efficiency; Reciprocity theorem

1. Introduction

The analysis of solar cell performance in terms of material and microscopic device parameters is the key to understanding device performance and efficiency. In general, two principal sets of electrical characteristics are used to consider cell performance: the *I–V* curve and the spectral response (SR). The *I–V* curve gives the fundamental parameters of the cell, i.e. short circuit current, open circuit voltage, fill factor and the cell efficiency. In addition, it also gives information regarding losses due to the internal resistances such as shunt and series resistances. The SR provides us with a more detailed insight since it tells us how the cell responds to the incoming photon fluxes in each device region. It also contains the richest information such as surface recombination velocities and the minority carrier diffusion length, which indicate the quality of the cell and the fabrication process [1–3].

Typically, the SR or, equivalently, the quantum efficiency (QE) is presented as a function of wavelength. However, it was suggested by Sinkkonen et al. [4] and further investigated by Donolato [2] that considering this parameter as a function of the absorption coefficient or distance will give a new interpretation that includes important information on the cell parameters such as diffusion length, junction depth, surface recombination velocity, etc.

When monochromatic light is normally incident on an infinitely thick cell, it is absorbed and attenuated by a factor $\exp(-\alpha(\lambda)x)$, where α is the absorption coefficient of the material under consideration, λ is the wavelength and x is the distance from the front surface. The response of the cell at any x position is related to the collection efficiency of charge carriers, $\eta_c(x)$, and can be written as

$$\mathrm{IQE}(\alpha) = \alpha \int_0^\infty \exp(-\alpha x)\eta_c(x)\,\mathrm{d}x. \quad (1)$$

The parameter $\eta_c(x)$ is sometimes called the spatial collection efficiency, for example by Sinkkonen et al. [4], or the collection probability, for example by Donolato [2], Green [5] and Brendel and Rau [6].

In earlier works, the parameter $\eta_c(x)$ has been derived by various methods. Sinkkonen et al. [4] used the inverse Laplace transformation to derive this parameter from the measured SR function. Donolato [2] proposed an

*Corresponding author. Tel.: +44 23 80592443; fax: +44 23 80593016.
E-mail address: patty@soton.ac.uk (P. Kittidachachan).

0927-0248/$ - see front matter © 2006 Elsevier B.V. All rights reserved.
doi:10.1016/j.solmat.2006.08.002

alternative way to derive this parameter by employing a deconvolution method.

In the present work, this parameter is considered in a different way based on the use of the diffusion equation for minority carriers derived by del Alamo and Swanson [7] and a reciprocity relationship between the charge collection and the dark carrier distribution [5,8–12]. The results obtained from the calculation are applied to study the performance of a solar cell. As will be shown in the following section, fitting the computed IQE derived from the collection efficiency with the experimental data allows the diffusion length, junction depth, and surface recombination velocities to be obtained.

2. Analytical methodology

In this work, the analysis of the emitter and base performance is based on a detailed consideration of the collection efficiency in the quasi-neutral regions of the base or the emitter; the collection efficiency from the depletion region is assumed to be unity.

To determine the collection efficiency of minority carriers within a non-uniformly doped emitter, the transport equations ((2) and (3)) are solved in the manner described in Refs. [5,7,8]. For simplicity of the analysis, the authors consider the charge carrier transport to be one-dimensional along a linear coordinate x, and the injected minority carrier densities to be small compared to the majority carrier densities, i.e., low injection assumption.

$$J_p = q\mu_p pE - qD_p \frac{\mathrm{d}p}{\mathrm{d}x}, \tag{2}$$

$$\frac{1}{q}\frac{\mathrm{d}J_p}{\mathrm{d}x} = G - \frac{1}{\tau_p}(p - p_0), \tag{3}$$

where J_p is hole current density; q is the electronic charge; μ_p, mobility of holes; E, Electric field; D_p, diffusivity of holes; G, carrier generation rate; τ_p, minority carrier lifetime of holes; p and p_0 are carrier concentration and carrier concentration at equilibrium, respectively.

For heavily doped regions, the $p_0(x)$ is modified to take into account of band gap narrowing:

$$p_0(x) = \frac{n_{\mathrm{ie}}^2}{N_{\mathrm{D}}} = \frac{n_{\mathrm{io}}^2}{N_{\mathrm{Deff}}}, \tag{4}$$

$$n_{\mathrm{ie}}^2(x) = n_{\mathrm{io}}^2 \exp\left(\frac{\Delta E_{\mathrm{g}}}{kT}\right). \tag{5}$$

where n_{ie} and n_{io} are the intrinsic carrier concentration and effective intrinsic concentration, respectively, N_{D} and N_{Deff} are the doping concentration and effective doping concentration, and ΔE_{g} is the apparent band gap narrowing.

A more convenient form of Eqs. (2) and (3) can be obtained by introducing the normalized excess minority-carrier concentration, $u(x)$ by

$$u(x) = \frac{p(x) - p_0(x)}{p_0(x)}. \tag{6}$$

The transport equation for the minority carriers in the dark can then be written as

$$-\frac{\mathrm{d}}{\mathrm{d}x}\left[D_p p_0 \frac{\mathrm{d}u}{\mathrm{d}x}\right] + \frac{D_p p_0}{L_p^2} u = 0. \tag{7}$$

where D_p is the hole diffusion coefficient, $L_p = \sqrt{D_p \tau_p}$ is the diffusion length, and τ_p is the hole lifetime. The reciprocity theorem (see, for example [8]) then states that the collection efficiency η_{c} is the solution of Eq. (7) with the boundary conditions $\eta_{\mathrm{c}} = 1$ at the junction edge and

$$qDp_0 \frac{\mathrm{d}\eta_{\mathrm{c}}}{\mathrm{d}x} = -J_{0S}\eta_{\mathrm{c}}, \tag{8}$$

at the surface, where S is the surface recombination velocity and $J_{0S} = qSp_0$.

Eq. (7) is manifestly in the self-adjoint (Sturm–Liouville) form and the reciprocity theorem follows directly [5].

The present method relies on the use of non-degenerate (Boltzmann) statistics, taking into account possible degeneracy through the use of effective band gap narrowing in Eqs. (4) and (5). The accuracy of this approach has been demonstrated on a number of occasions [7,13] although, if higher accuracy is desired, the full numerical solution with Fermi–Dirac statistics can be used, albeit at the cost of substantially increased complexity [14]. Auger recombination, which occurs at high doping densities, is included through an appropriate term in the minority-carrier lifetime (the N_{D}^2 term in Table 1).

The determination of u or η_{c} for the emitter must, in general, be carried out by numerical quadrature on account of the non-uniform doping and heavy doping effects. To separate the effect of surface from bulk recombination it is convenient to follow del Alamo and Swanson [7] and define the "forward" and "reverse" solutions u_{f} and u_{r} of Eq. (7) with the following boundary conditions:

$$u_{\mathrm{f}}(0) = 0; \quad u_{\mathrm{f}}(W_{\mathrm{e}}) = 1, \tag{9}$$

$$u_{\mathrm{r}}(0) = 1; \quad u_{\mathrm{r}}(W_{\mathrm{e}}) = 0, \tag{10}$$

where $x = 0$ and $x = W_{\mathrm{e}}$ correspond to the surface of the emitter and the junction edge, respectively. With the help of u_{f} and u_{r}, it is easy to show that the collection efficiency in the emitter which satisfies the correct boundary conditions is given by

$$\eta_{\mathrm{c}}(x) = u_{\mathrm{f}}(x) + \frac{\alpha_{\mathrm{r}} J_{0\mathrm{r}}}{J_{0\mathrm{r}} + J_{0S_{\mathrm{e}}}} u_{\mathrm{r}}(x), \tag{11}$$

where $J_{0S_{\mathrm{e}}}$ refers to surface saturation current density,

$$J_{0S_{\mathrm{e}}} = \frac{qn_{\mathrm{i0}}^2 S_{\mathrm{e}}}{N_{\mathrm{Deff}}(W)}, \tag{12}$$

Table 1
Parameters used for modelling [13]

Parameters	Details	Unit
Energy band gap narrowing	$\Delta E_g = 14 \times 10^{-3} \times \left[\ln\left(\frac{N_D}{1.4\times10^{17}}\right)\right]$	eV
Minority carrier lifetime	$\tau = \left[50 + (2 \times 10^{-13} \times N_D) + (2.2 \times 10^{-31} \times N_D^2)\right]^{-1}$	s
Hole mobility	$\mu_p = 155 + \frac{315}{1+\left(N_D/10^{17}\right)^{0.9}}$	$cm^2\,V^{-1}\,s^{-1}$

S_e is surface recombination velocity at the front surface, and

$$J_{0r} = qDp_0 \left.\frac{du_r}{dx}\right|_{x=0} \quad \alpha_r J_{0r} = qD_p p_0 \left.\frac{du_r}{dx}\right|_{x=W}. \tag{13}$$

It should be stressed that although the solutions u_f and u_r are determined numerically they can aside from the low-injection approximation, be considered exact. Therefore they can be obtained without the need for a series expansion or the transparent/quasi-transparent approximations.

For the p-type base region, the determination of the collection efficiency is straightforward because the doping can be assumed to be uniform; the presence of the back surface field can be allowed for in the value of the surface recombination velocity S_b at the back surface. One then readily finds

$$\eta_c(x) = \cosh(x/L_n) - \frac{\tanh(W_b/L_n) + S_b L_n/D_n}{1 + (S_b L_n/D_n)\tanh(W_b/L_n)} \sinh(x/L_n), \tag{14}$$

where W_b is the base width, x is measured from the junction edge, and the subscripts of L_n and D_n refer to the appropriate quantities for electrons in the p-type base.

In the present analysis, the IQE of the device was determined from the following relations:

$$\mathrm{IQE} = \frac{1}{1-R}\,\mathrm{EQE}, \tag{15}$$

where reflectance R now includes the possibility of internal reflections within the device (EQE—external quantum efficiency).

$$R = \frac{(1-R_{fe})R_b(1-R_{fi})e^{-2\alpha W}}{1 - RR_{fi}e^{-2\alpha W}} + R_{fe}. \tag{16}$$

The EQE was determined from

$$\mathrm{EQE} = \int_0^W \eta_c(x) g(x)\,dx, \tag{17}$$

and the generation function $g(x)$ that was employed in the model is

$$g(x) = \frac{\alpha(1-R_{fe})}{1 - R_b R_{fi} e^{-2\alpha W}} \{e^{-\alpha x} + R_b e^{-2\alpha W} e^{\alpha x}\}, \tag{18}$$

where R_{fe} is the external front surface reflectance; R_{fi} is the internal front surface reflectance; R_b is the reflectance at the back surface of the device and W is the thickness of the cell. The absorption coefficient was taken from Ref. [15]. Eqs. (15) and (18) are the results of a standard analysis for a planar solar cell with a back surface reflector. It was found that a better fit to the data near the silicon band gap could only be achieved using different values of external and internal front surface reflectance. This can easily be explained in terms of small variations in the orientation of the back contact along the solar cell, resulting in small variations in the angle of internal incidence onto the front surface. This will result in a marked increase in the internal reflection coefficient as some of the rays will now fall outside the escape cone and undergo total internal reflection.

3. Sample preparation and characterization

To demonstrate the applicability of the analytical approach, we have used it to analyze performance as a function of location within the body of an $n^+/p/p^+$ c-Si solar cell. The cell used in this study was fabricated at Innos Ltd., as part of a development batch designed to study the effect of emitter diffusion on the device performance.

The starting material was p-type Wacker float-zone silicon with a doping concentration corresponding to 1–3 Ω cm. The thickness of the wafers used was 416 ± 0.1 μm and the crystal orientation was ⟨1 0 0⟩. The wafers were single sided polished and 100 mm in diameter. The wafers were cleaned by the RCA cleaning process and the front surface was passivated with a 400 nm thick thermal oxide. The back surface of the substrate was diffused with boron using "Boron Plus" solid source tiles to create a p^+ layer back surface field (BSF). The boron was diffused at a temperature of 1050 °C using in a nitrogen and dry oxygen atmosphere. The active area was defined to be 1 cm^2 by photolithography. An n^+ emitter layer was formed on the front surface by phosphorus diffusion using "Phosplus" solid source tiles at 1000 °C for 30 min. Following this, a thin layer of SiO_2 was deposited on the wafer front surface by LTO deposition. This provides an antireflective layer with a minimum reflectance around 8.8% at a wavelength of 620 ± 10 nm and a total reflectance of approximately 16% over the 400–1000 nm range. To form the n-type contact, windows were opened in the oxide using a photolithographic process. A sequence of

Ti–Al layers was then evaporated onto the front to form a front grid contact pattern with a total thickness of 600 nm and a shading loss of 5%. The p-type contact was formed by evaporating 1000 nm of aluminum onto the rear of the wafer. The contacts were annealed in H_2/N_2 ambient at a temperature of 450 °C for 15 min in order to reduce the contact resistance between the metal and semiconductor.

4. Results and discussion

The doping profile of the emitter, which presents only the electrically active carriers, was measured using the spreading resistance profiling (SRP) technique. The emitter doping profile for the calculation was obtained by a polynomial fit of the SRP data. Both profiles were plotted together as shown in Fig. 1. The comparison indicates that the doping profile generated from the polynomial function is in good agreement with the profile obtained from the measurement.

The modeled result, which presents the collection efficiency within the emitter as a function of the distance from the front surface and the surface recombination velocity (SRV) is shown in Fig. 2. The plot indicates that the collection efficiency increases towards the junction boundary and has a value close to unity at the junction edge. The plot also suggests that the collection efficiency

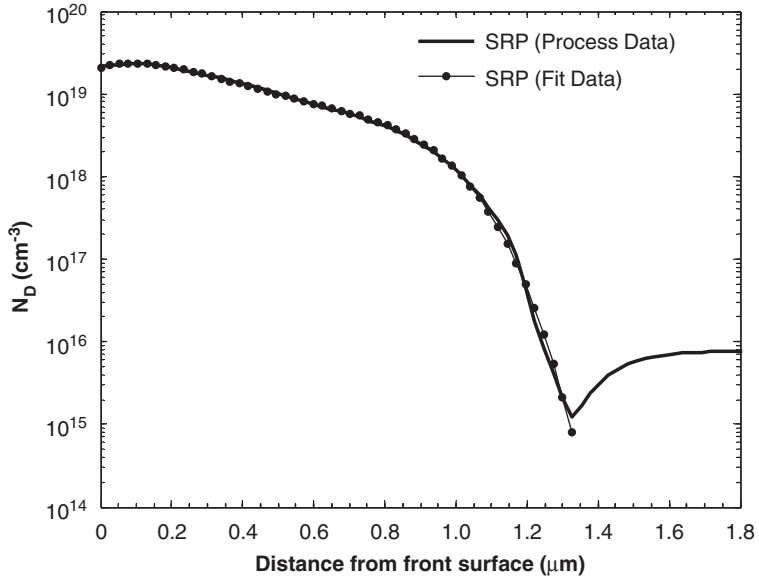

Fig. 1. Comparison of SRP profiles obtained from measurement and fitting. ($N_s = 2 \times 10^{19}\,cm^{-3}$, $N_a = 8 \times 10^{15}\,cm^{-3}$, $x_j = 1.30\,\mu m$).

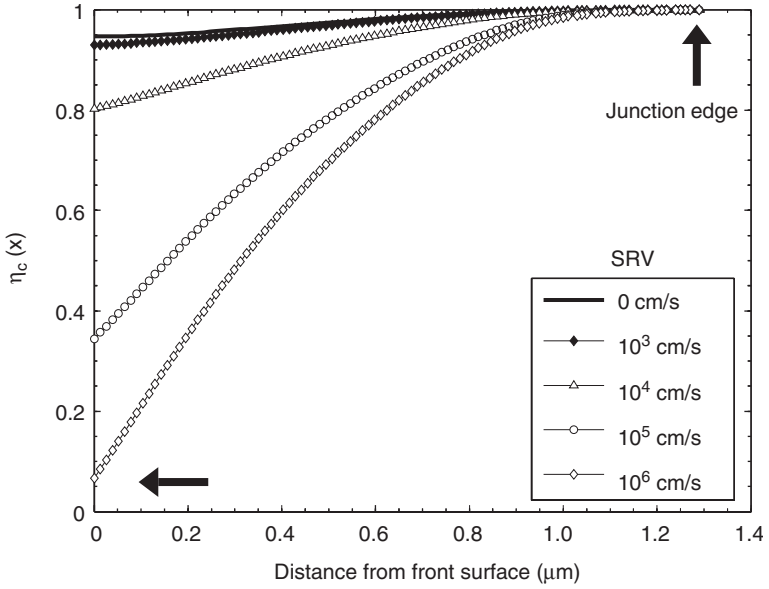

Fig. 2. The minority carrier collection efficiency within the emitter, calculated from the SRP profile. The arrow indicates the curve for $S = 10^6\,cm\,s^{-1}$ as used for the curve fitting for the present solar cell.

depends strongly on the surface recombination velocity and it drops dramatically as S_e becomes higher than $10^3\,cm\,s^{-1}$.

The doping concentration in the base region was considered to be uniform and from the SRP data presented in Fig. 1, it is equal to $8\times10^{15}\,cm^{-3}$. The collection efficiency calculated from (14) for different values of the surface recombination velocity is shown in Fig. 3. As can be seen from the plot, the collection efficiency increases towards the junction boundary and is highest at the junction edge. The collection efficiency at the back surface decreases from 0.63 to 0.33 as S_b increases from 0 to $10^3\,cm\,s^{-1}$.

Fig. 4 shows a comparison of the experimental IQE (tested by NREL under AM1.5 ($1\,kW\,m^{-2}$) spectrum at an ambient temperature of 25.0 °C) with the results calculated from the present model and PC1D (Ver. 5.3). The experimental IQE was determined from Eq. (15).

Table 2
The cell parameters chosen for the simulations

Parameters	Present model	PC1D	Unit
Emitter surface concentration	2×10^{19}	2×10^{19}	cm^{-3}
Base doping concentration	8×10^{15}	8×10^{15}	cm^{-3}
Junction depth	1.35	1.35	μm
Front SRV	10^6	10^6	$cm\,s^{-1}$
Back SRV	250	250	$cm\,s^{-1}$
Electron diffusion length	747	747	μm
R_b	75	75	%
R_f	69	69	%

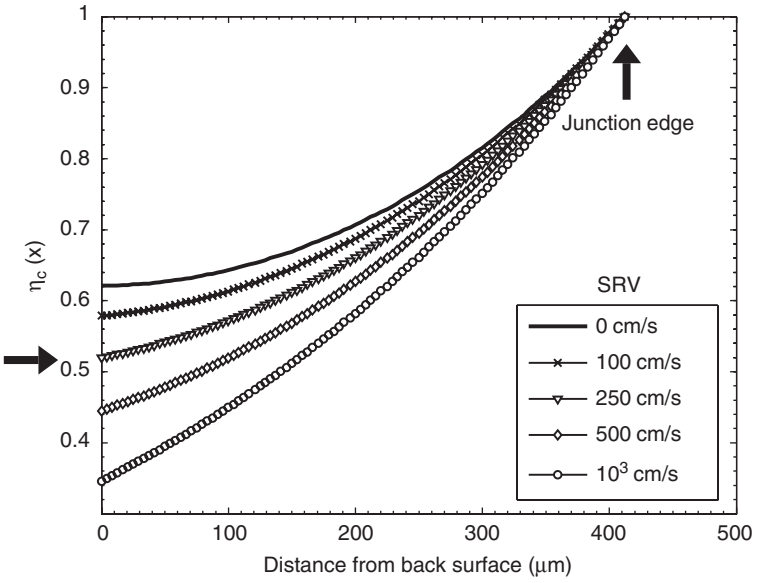

Fig. 3. The minority carrier collection efficiency within the base. ($L = 747\,\mu m$). The arrow indicates the curve for $S = 250\,cm\,s^{-1}$ as used for the curve fitting for the present solar cell.

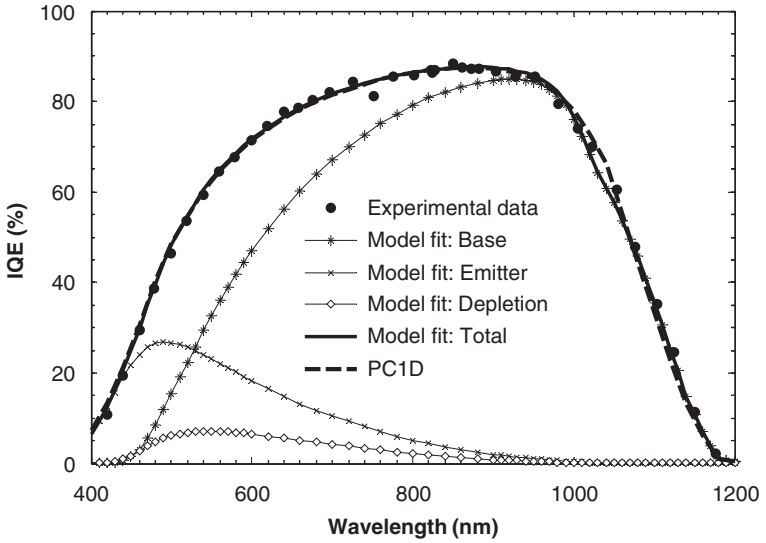

Fig. 4. Comparison of internal quantum efficiency from the model and experimental data.

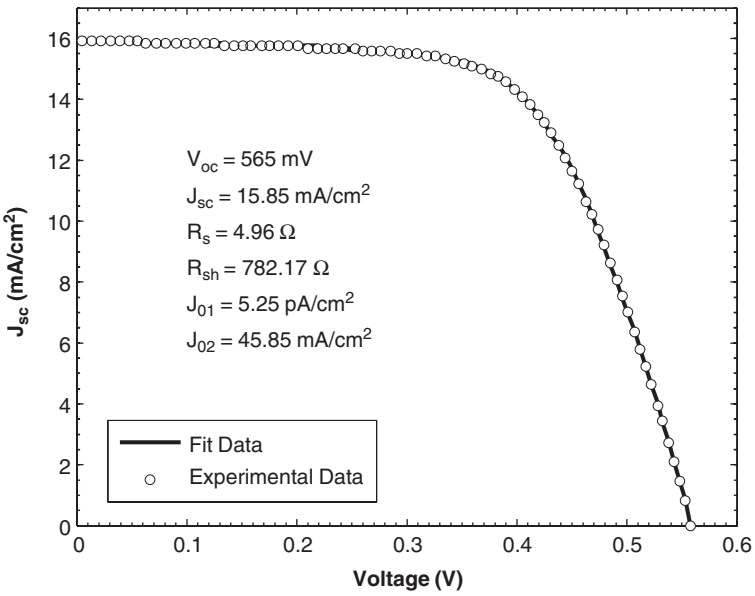

Fig. 5. *I–V* characteristic of the cell. The fitted data from the two-diode model is also shown for comparison.

The cell parameters chosen for the simulation for the present model and PC1D are summarized in Table 2. It should be noted that the results obtained from our calculation are in good agreement with the simulated result obtained from PC1D. A slight disagreement is probably due to differences in the optical models, which, in the present calculation takes into account internal reflection but does not allow for light trapping effects, which are included in PC1D [16]. Unlike PC1D, the procedure suggested in this paper makes it possible to separate contributions not only from indicated regions of the cell as in Fig. 4, but from separate parts of each region through the collection efficiency (Figs. 2 and 3) The fitted parameters also suggest that the device has a high front surface recombination velocity and low back surface recombination velocity. These results reveal that the technological process for passivating the front layer still need to be further developed in order to enhance the collection efficiency from the emitter. The BSF structure effectively minimizes the surface recombination velocity at the back surface of the devices.

The present model is designed specifically to predict the cell quantum efficiency. For completeness, however, Fig 5 shows a fit to complete *I–V* characteristic of the cell considered in this approach.

The experimental *I–V* data was tested by NREL at AM1.5 and an ambient temperature of 25.0 °C. Under these test conditions, the cell has V_{oc} of 564.8 mV, J_{sc} of 15.94 mA cm^{-2}, FF of 63.45%, and η of 5.71%. The extracted parameters after fitting of the curve based on the use of the two-diode model are also shown in the figure. We note that these results also indicate areas where further work is required to improve performance.

5. Conclusions

The performance of a p–n junction solar cell was studied experimentally and theoretically in terms of collection efficiency in each region. The collection efficiency of the emitter was derived by considering the diffusion equation for minority carriers and a reciprocity relationship of the charge collection and the dark carrier distribution. The collection efficiency of the base was studied analytically.

For comparison, we have also fitted the internal quantum efficiency obtained from the model with the experimental data and extracted important cell parameters. These parameters include front and back surface recombination velocities, the minority carrier diffusion lengths and the junction depth.

The fitted results show that the good response from the base region is due to an adequate diffusion length and a very good back surface field, which leads to very low effective surface recombination velocity at the back surface. The poor response of the cell at short wavelength is due to a high front surface recombination velocity. Good surface passivation therefore needs to be applied to improve both the blue response and the open circuit voltage.

Acknowledgments

The authors would like to thank Paul Basore for useful discussion about fitting experimental data with PC1D program. We are also grateful to Dr. Keith Emery and Tom Moriarty of NREL for their help with cell characterization. Pattareeya Kittidachachan acknowledges the financial support from Royal Thai Government

throughout her PhD studies. Project supported in part by the EPSRC Supergen Program.

References

[1] S.M. Sze, Physics of Semiconductor Devices, Wiley, New York, 1981.
[2] C. Donolato, J. Appl. Phys. 89 (2001) 5687.
[3] P.K. Singh, R. Kumar, P.N. Vinod, B.C. Chakravarty, S.N. Singh, Sol. Energy Mater. Sol. Cells. 80 (2003) 21.
[4] J. Sinkkonen, A. Hovinen, T. Siirtola, E. Tuominen, M. Acerbis, in: The Paper Presented at the Proceedings of the 25th IEEE Photovoltaic Specialist Conference, Washington, DC, 1996.
[5] M.A. Green, J. Appl. Phys. 81 (1997) 268.
[6] R. Brendel, U. Rau, J. Appl. Phys. 85 (1999) 3634.
[7] J. del Alamo, R.M. Swanson, IEEE Trans. Electron. Devices ED-31 (1984) 1878.
[8] T. Markvart, IEEE Trans. Electron. Devices ED-43 (1996) 1034.
[9] T. Markvart, IEEE Trans. Electron. Devices 44 (1997) 1182.
[10] C. Donolato, Appl. Phys. Lett. 46 (1985) 270.
[11] U. Rau, R. Brendel, J. Appl. Phys. 84 (1998) 6412.
[12] K. Misiakos, F.A. Lindholm, J. Appl. Phys. 58 (1985) 4743.
[13] A. Cuevas, P.A. Basore, G. Girouit-Matlakowski, C. Dubois, J. Appl. Phys. 80 (1996) 3370.
[14] P.P. Altermatt, J.O. Schumacher, A. Cuevas, M.J. Kerr, S.W. Glunz, R.R. King, G. Heiser, A. Schenk, J. Appl. Phys. 92 (2002) 3187.
[15] M.A. Green, High Efficiency Silicon Solar Cells, Trans. Tech., Aedermanndorf, Switzerland, 1987, p. 228.
[16] P.A. Basore, in: Proceedings of the 23rd IEEE Photovoltaic Specialists Conference, IEEE, New York, 1993, p. 147.